Benefits of non-linear structural analysis for optimising the seismic assessment and retrofitting of a CEA laboratory

Quentin Haessler, Fabien Mémeteau, Jean-Marc Vezin, Etienne Guitton, Xavier Pinelli

Benefits of non-linear structural analysis for optimising the seismic assessment and retrofitting of a CEA laboratory

Quentin Haessler Fabien Mémeteau CEA Centre de Cadarache 13108 Saint-Paul-lez-Durance quentin.haessler@cea.fr / fabien.memeteau@cea.fr	Jean-Marc Vezin Etienne Guitton Sixense necs 196 rue Houdan 92330 Sceaux - France jean-marc.vezin@necs.fr / etienne.guitton@necs.fr	Xavier Pinelli LMPS - ENS Paris Saclay 4 avenue des Sciences 91190 Gif-sur-Yvette - France xavier.pinelli@ens-paris-saclay.fr

Abstract:

Within the scope of extending the service life of a CEA nuclear facility, a seismic assessment using non-linear transient analysis was carried out between 2017 and 2019. The facility in question was built in the early sixties and was not designed to resist earthquake loads. In the early 2000s, its utilities and engineered structures were refurbished to meet the design requirements of a plausible historically maximum earthquake (PHME).

About ten years later, it was decided to continue the activities in this facility beyond the duration that was initially defined following the refurbishment work completed in the early 2000s. Therefore further seismic assessments were initiated to identify any other engineered structures reinforcement required to resist an earthquake combining the effects of both a safe shutdown earthquake and a paleo-earthquake.

A test campaign was carried out to collect the data needed to develop a more refined model of the behaviour of some reinforcement work completed in the 2000s to meet the PHME requirements.

These new seismic assessments used non-linear transient dynamic analysis to consider the behaviour of reinforced concrete, incorporating the results of the test campaign, the possible uplift of the columns' footings, and the in-plane and out-of-plan behaviour of the masonry panels.

This article describes the context of the facility subject to these seismic studies, followed by the objectives, methodology and design assumptions. It then details the modelling with respect to the characterisation test results, the implementation of these results, and the local calculations performed to both precisely define the strengthening's works needed and to demonstrate structural stability and resistance. Lastly, the programme of strengthening's works' defined on the basis of these studies is presented.

KEYWORDS:

Seismic study, nuclear facility, non-linear transient analysis, strengthening's works, characterisation tests

1. General context

As part of extending the service life of a CEA nuclear facility, a seismic assessment using non-linear transient analysis was performed between 2017 and 2019 to take into account the combined effects of a safe shutdown earthquake and a paleo-earthquake. A test campaign was carried out to define certain parameters needed to develop a refined model of the behaviour of some reinforcements made to the facility in the early 2000s to meet the design requirements of a plausible historically maximum earthquake (PHME).

This article first describes the building concerned by these seismic assessments. It then explains the tests carried out to characterise the behaviour of the existing reinforcements. The seismic assessments are detailed thereafter, specifying the combination of actions chosen, the methodology applied, the configurations analysed (number of seismic signals, stiffness of the support bearings and structural components, behaviour laws), and the results analysed with our interpretation. Lastly, the article describes the programme of the strengthening's work defined on the basis of these results.

2. Description of the building and historical context

The facility in question was built on a rocky subsoil in the early sixties. The building comprises a reinforced concrete frame that is 80 metres long and 36 metres wide. It has three levels, i.e. basement, ground floor and first floor.

The central part of the roof (+14.50 m) is higher than its two side parts (+6.69 m). The building is divided into three separate blocks of equal length, with an expansion joint installed between the superstructures.

The engineered structures were initially not designed to resist earthquake conditions.

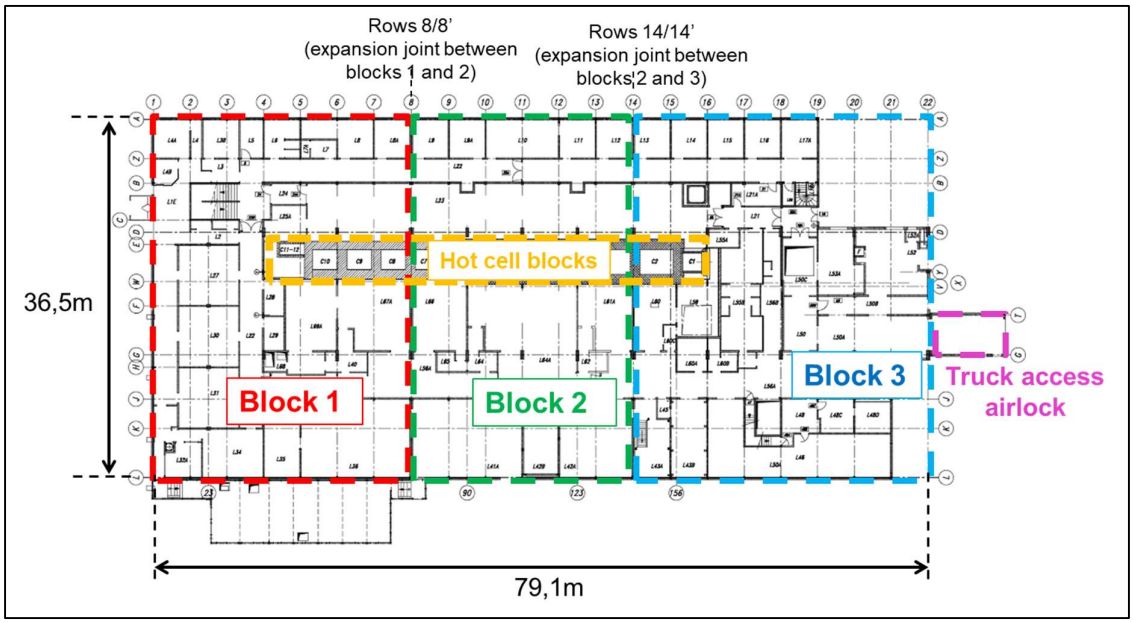

Figure 1 – Floor plan of the ground level

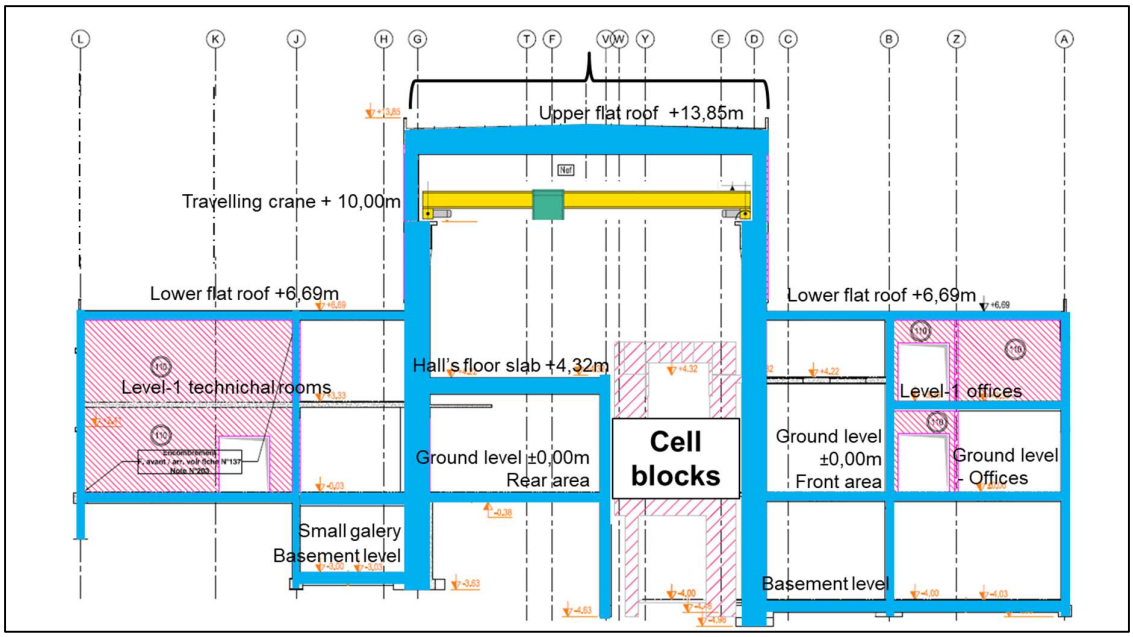

Figure 2 – Cross-sectional view of the building

The utilities were refurbished and the engineered structures strengthened in the early 2000s to meet the design requirements of a plausible historically maximum earthquake (PHME). The structural reinforcements and changes made it possible to improve the building's overall seismic behaviour, such as eliminating the risk of interactions inside the building, eliminating loads, masses and rigid points, creating of new bearing points and increasing its overall structural strength.

The strengthening's works having allowed these improvements are described in Appendix 1.

3. Characterisation of the strengthening's works done to meet PHME requirements

In addition to the studies described in Section 4, a series of mechanical tests was carried out to validate:

- Bending and shear behaviour of the reinforced concrete structures strengthened with bolted-bonded sheet metal.
- Behaviour and resistance of the coupling devices (bolted sheet metal) on the concrete structures between blocks 1, 2 and 3.

3.1 - Tests to check the behaviour of bolted-bonded sheet metal strengthening

Considering the fact that the hall's columns play a crucial role in the bracing and seismic resistance of the structure, it was decided to test specimens that are representative of those.

The initial construction provisions and PHME strengthening's works on these columns were analysed before producing the test samples. Analysis indicated that samples representative of columns from rows 8-8' and 14-14' needed to be tested.

Predictive resistance calculations of the strengthened test samples were obtained using a multifibre beam model.

3.1.1 - Tests to validate the strengthening's process in the main areas

In terms of the bending strength (4-point bending test) and shear strength (3-point bending test), a batch of non-strengthened test samples (F0 and C0) with the same formwork and concrete reinforcement as the strengthened samples was subjected to the same support and load conditions. Our objective was to quantify the increased resistance and ductility of the strengthened test samples (FR1 and CR) thanks to the strengthening's process.

3.1.2 - Tests to validate the strengthening's process for singularities

In terms of the bending strength, three additional samples (called FR2) were tested under the same load conditions as those for the F0 and FR1 samples in order to validate the behaviour of coupling systems (external rods installed perpendicular to the floor between sections of strengthened columns).

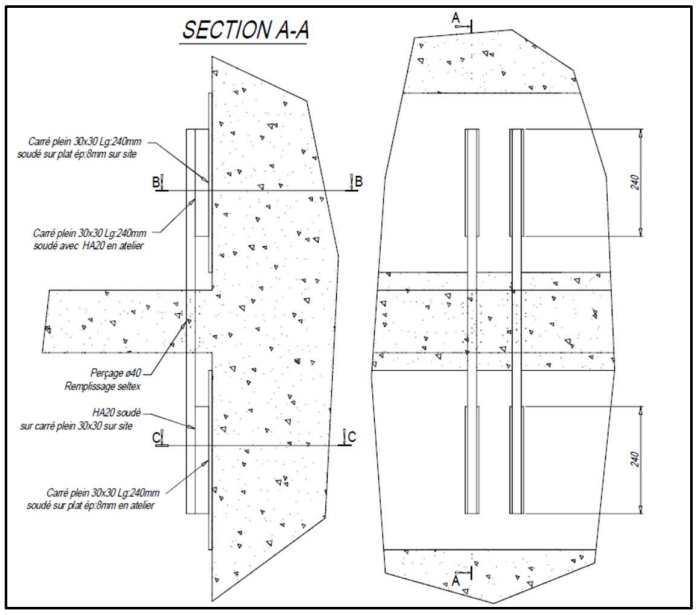

Coupling system perpendicular to the floor (extract of drawing)

We tested samples (called J) representative of the cover-strips, which are bolted-bonded metal plates installed by section and connected by metal plates that are welded to the end of each section.

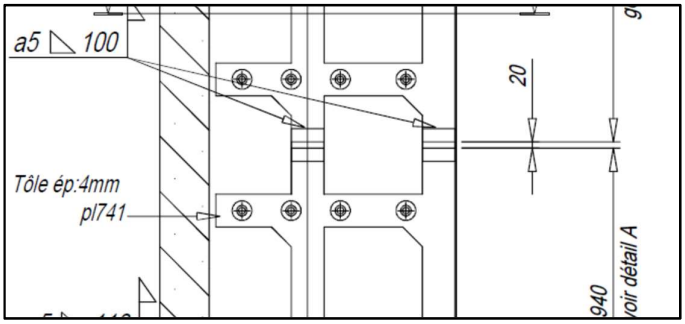

Cover-strips between sections (extract of drawing)

3.1.3 - Impact of tests on modelling of the sections strengthened by bolted-bonded metal plates

3.1.3.1 - Bending tests F0, FR1 and FR2

• Observations and analysis:

The tests were reproducible and there was very little scatter in the results.

The strengthening's measures are therefore confirmed to be effective:

- The strength of the strengthened beams is tripled compared with that of the non-strengthened beams, complying with our predictive calculations
- The ductility of the strengthened beams is also satisfactory. No brittle failure mode was observed, other than the fracture of a weld at the joint between the 4 and 8 mm metal plates for the FR2 test samples (see NB below). More specifically, no bolt failure or excessive slip was detected
- The FR2 tests show that the coupling of metal plates using external rods ensures continuity between the reinforcements through the floor, rendering the beams stronger than the reinforcements in the main areas on the condition that the welds have been strengthened (see NB below).

NB: The first test sample, FR2_3, suddenly failed at two-thirds of the maximum load applied during tests on the FR1 samples. This fracture occurred because the weld was undersized and the metal plates were not cut in a way to transfer the tensile force between metal plates of very different thicknesses (no taper). The tests on the FR2_1 samples – whose joining areas between 4 and 8 mm metal plates were reinforced with welded splices – revealed a comparable level of strength and ductility that was sometimes even greater than the FR1 samples. The FR2_1 test also made it possible to validate a solution for consolidating the welds in question.

The tests on the FR1 samples showed that adhesive could not be used to provide bucking resistance. In the case of the third FR1 sample tested, i.e. FR1_1, the metal plates located in the central area of the sample and subjected to compressive stress (top part of the beam cross-section) were pinned to the concrete (8 pins spaced 40 cm apart). These pins limited buckling in the plates, though without a clearly positive effect on the failure load compared with the two other samples - FR1_2 and FR1_3 - that were tested without pins.

• Impact on the bolted-bonded metal plate strengthening's process

In light of the above, the welds between 4 and 8 mm thick metal plates located at the base and top of the beam sections strengthened by bolted-bonded plates needed to be reinforced by splices.

The risk of buckling in metal plates subjected to compressive stress was incorporated into the behaviour law that was applied to model the non-linear behaviour of reinforced concrete sections in our strength analysis studies (see Section 4.1).

• Impact on the modelling of sections strengthened by bolted-bonded metal plates

The comparison of test results with the non-linear calculation results was used to check the overall validity of the multifibre beam model for reinforced columns and beams, as well as the similarity in behaviour with a section of reinforced concrete.

Analysis of the test results also allowed us to identify improvements that could be made to the behaviour law used on the metal plates in order to take into account:

- Metal plate slip between bolts by reducing Young's modulus
- Buckling in compressed metal plates by applying a different behaviour law with respect to compression.

These improvements have been incorporated into the structural strength analysis described in section 4.1.

3.1.3.2 - Shear tests C0 and CR

• Observations and analysis:

Cracks were observed in the CR strengthened test samples at loads between 300 and 400 kN, i.e. about twice the cracking load for the C0 samples.

Cracking was also more evenly distributed in the CR strengthened test samples than in the C0 non-strengthened samples.

A mean shear strength of 268 kN was determined for the three CR test samples (values between 250 and 292 kN). Scatter was very low (between -7% and 9%), even though it is higher for the shear tests on the C0 non-strengthened beams.

The shear strength is significantly improved for the samples strengthened with bolted metal plates. The increase in the shear strength is between 152 and 250 kN, i.e. +64%, based on the minimum values of the three tests.

The ductility of the strengthened beams is also improved with respect to shear: the drop in resistance for the CR samples after the peak load is slower. The improved ductility is most probably due to the better distribution of cracks and thus of deformation. The cracks in the CR samples were also not as wide as those in the non-strengthened C0 samples, thereby maintaining better resistance to friction over a broader range of deformation.

• Impact with respect to the improved shear strength of the strengthening's process

Analysis of the test curves for the CR samples and the strength model based on the limit-state design rules for reinforced concrete were both used to estimate the improved shear strength provided by the straps installed perpendicular to the longitudinal axis of the test samples under the following conditions:

- Straps perpendicular to the longitudinal axis of the beam are likened to transverse reinforcement (such as frames or brackets)
- The effective tensile stress area of these straps is limited by the anchoring capacity of the bolts.

3.1.3.3 - J tensile tests

• Observations and analysis:

Six samples were manufactured, including three according the process used for PHME strengthening's works (MAG 135).

Five samples (3 welded with tungsten inert gas and 2 with metal active gas) reached the maximum jack load, i.e. 300 kN, without showing any signs of failure.

Sample ref. MAG J-4 showed the beginnings of a fracture in a weld but it nonetheless reached a maximum load of 292 kN with no downward phase.

The tests showed good reproducibility, including for the J-4 sample.

An elastic phase can be observed up to a load of about 200 kN before the curve changes direction, most probably indicative of plastic deformation in the metal plates due to the bending with axial force.

It can then be seen that the load increases up to the end of the test and the resulting deformation ranges between 0.8% and 1.7%. The behaviour can therefore be qualified as relatively ductile.

• Impact on the strength calculation checks

The minimum strength measured across all the tests was 292 kN, i.e. a mean tensile stress of 365 MPa in the metal plates, which exceeds the elastic limit of S355 steel.

The strength of the welded cover-strips is therefore sufficient to subject the metal plates to a load up to their elastic limit without the risk of brittle failure.

However, as the beginnings of a fracture could be observed in one of the samples, we checked on the basis of calculations using non-linear transient analysis that the stress in the metal plates remained below 292 MPa in areas equipped with cover-strips, i.e. calling for a safety factor of 1.25 (consistent with the γ_{M2} safety factor given in Eurocode 3).

3.2 – Tests to check the behaviour of coupling devices

To determine the strength and ductility of the bolts embedded in reinforced concrete components comprising some of the existing coupling devices, samples G1 and G2 were manufactured and tested under tensile conditions during which the bolts were subjected to shear.

Analysis of these tests showed relatively small scatter for both types of samples.

It was shown that the bolts were very ductile. Their failure occurred during their removal/ slip from their embedding in the concrete.

Except for the G1 sample, all the bolts were removed without any fracture in the metal, and no deformation could be seen in the bolt heads and their welds on the connecting washers with the metal plates.

The behaviour law applied to the embedded HA bolts called HA8 and HA12 was likened to an elastic-plastic linear strain-hardening law, incorporated in the non-linear model for the coupling devices in question.

4. Seismic behaviour assessment

The seismic behaviour of the structure was investigated using global 3D finite-element modelling based on non-linear transient analysis. This was necessary to take into account the non-linear behaviour of reinforced concrete structures in order to establish the most realistic representation of the building's seismic response. Two types of earthquakes were studied with respect to the seismic risks at the Cadarache site: safe shutdown earthquake and paleo-earthquake.

4.1 – Modelling and non-linear behaviour laws

The *Code_Aster* model used for the study was based on a model developed for the *Hercule* software during the previous strengthening's studies. The building is therefore represented in its current state, i.e. with the strengthening's works done to meet the PHME requirements. The modelling includes the structures forming the three main blocks of the building and the truck access airlock and their coupling mechanisms.

The types of finite elements were chosen according to the geometry of the structures represented:

- Flat components (walls and floors) were represented by thin shell elements
- Slender components (columns and beams) were represented by beam elements. The type of connection between components was adapted according to their effective capacity to transfer bending moments to their ends:
    - Components forming the main frame of the hall were fixed at both ends
    - Beams forming the frames of annexe buildings with a reduced bending capacity were first articulated at both ends. These hinges were then replaced by embedments because the modelling used made it explicitly possible to take into account realistic connections between components.
- Ribbed slabs were modelled by representing the ribs with beams, while the compression slab was represented by thin shells

- Masonry components likely to contribute to the stiffness of the overall system were modelled by macro-elements to represent their behaviour both in-plane and out-of-plane
- Coupling devices were modelled by beam elements with the different connections representative of the construction measures applied during the PHME strengthening's works
- The building's stack was modelled by thin shell elements
- Stairwells were modelled by stick models disconnected from the structures and adjacent floors in compliance with the separation measures implemented during the PHME strengthening's works.

The behaviour of the finite elements representing the stack, the stairwells, the truck airlock slab and the columns' footings in the hall was assumed to be linear elastic.

The elements most likely to fall in the post-elastic range were assumed to have non-linear behaviour, such as beam-column frame components, walls and slabs made from reinforced concrete (excepting the truck airlock slab), as well as masonry panels.

The types of elements used in the non-linear model of reinforced concrete were multi-layer shells to represent walls and multifibre beams to represent frame structures. The behaviour of concrete and that of its reinforcement were represented separately by distinct behaviour laws.

The non-linear behaviour of concrete was modelled by a law incorporating tensile and compression damage, which is very similar to the parabola-rectangular law.

The non-linear behaviour of reinforcement bars and metal plate reinforcements was modelled by an elastic-plastic law taking into account linear kinetic hardening.

The connections of coupling devices between blocks were first modelled by a linear behaviour law, then by non-linear behaviour laws based on the results of tests performed as part of the post-test loopback calculations (G1- G2 tensile tests).

This study included the contribution of masonry components to the building's bracing system, except when they:

- were disconnected from the frame (case of rows 4 and 22, and the walls in the rear area)
- included large-sized openings
- were not very thick (less than 11 cm).

The non-linear behaviour of masonry panels was modelled as follows:

- In-plane: a non-linear law representing the cyclical deterioration of the strength and stiffness was applied to the two compression rods along the two panel diagonals
- Out-of-plane: a standard failure criterion was taken into account in a simplified manner based on reaching a limit out-of-plane acceleration.

Two assumptions were applied in the calculations to take into account uncertainties affecting their stiffness and strength:

- Assumption of the maximum stiffness and strength values
- Assumption of the minimum stiffness and strength values.

The data collected from the tests were then incorporated by adapting the behaviour laws of the different components to include the test feedback, as described in Section 3. This mainly led to defining specific behaviour laws to represent the non-linear behaviour of the metal plate reinforcements and the coupling devices.

4.2 - Type of analysis and configurations studied

A non-linear transient analysis was performed for four different calculation configurations. Two earthquake assumptions were considered: safe shutdown earthquake and paleo-earthquake. Each earthquake assumption was associated with two masonry behaviour assumptions (minimum and maximum).

Each of the earthquakes was represented by a set of five decorrelated accelerograms. The 3D seismic movement was simulated by simultaneously applying three accelerograms - one in each direction - and

taking into account a weighting factor of two-thirds on the vertical component. Five simulations were performed by switching the accelerograms in a circular manner.

The initial internal damping of the structures was taken into account by implementing a damping matrix, C, using Rayleigh's method based on the linear combination of the mass and stiffness matrices: $C = \alpha M + \beta K$. From a conservative viewpoint, the coefficients α and β were defined to establish the damping level $\xi_1 = 2\%$ of the frequency $f_1 = 0.5$ Hz and damping level $\xi_2 = 5\%$ of the cut-off frequency $f_2 = 35$ Hz. This adjustment results in a damping level below 2% for the frequency range of [0.5 Hz -13 Hz], and a level between 2 and 5% for the frequency range of [13 Hz - 35 Hz]. The damping level is below 1% for the frequency range of [1.14 Hz - 5.90 Hz].

Additional damping results from damage to the materials, which occurs due to hysteresis associated with the non-linear behaviour laws governing materials (concrete and steel).

The overall effective damping of the model was controlled by analysing the attenuation of the free oscillations in the structure after the strong phase of the earthquake. The overall loads were also analysed. An overall effective damping value between 3 and 6% was obtained, which is conservative compared with the standard assumptions used in seismic calculations for reinforced concrete structures ($\xi = 7$ %).

The loads were applied in two phases. The permanent loads (gravity + pressure from backfill soil) were first applied as part of a static analysis. In the second phase, the seismic load comprised inertial force applied in all three directions and dynamic thrust from backfill soil. This load was applied and superimposed on the initial static load.

The time integration algorithm was based on the Hilbert, Hughes and Taylor (HHT) implicit method with a time step of about 0.01 seconds.

4.3 – Analysis and interpretation of results

To cover any uncertainties due to the variability of results depending on the accelerograms, and in compliance with ASN guidelines 2-01, the values representative of each parameter studied must be assessed according to the Student-Fisher law. We calculated the envelope value for each relevant parameter, G, and for each of the five sets of accelerograms. We then determined the envelope value representing all five sets of accelerograms by calculating the mean of the envelope values for all five sets + 0.95 x standard deviation. The envelope value of the results across all four calculation configurations could then be determined.

4.3.1 – Structural displacements

According to the results, the structures undergo significant displacements during a safe shutdown earthquake and paleo-earthquake, reaching between 11 to 17 cm for the roof in the north-south direction (along the X-axis horizontal to the hall) and 8 cm in the east-west direction (Y-axis longitudinally). Very significant local displacement also occurs in the gables of rows 4 and 22, and in the masonry panels of rows J-L/8, 11 and 14.

Displacements along the X-axis progressively increase with height, whereas displacements along the Y-axis are specifically concentrated down the height of the ground floor (up to 7 metres). This is because the masonry on the ground level parallel to the Y-axis is reaching its failure point, which results in greater flexibility in this level whereas the masonry in the higher levels of the building retains its properties and experiences less deformation.

The non-linear transient analysis calculated displacement to be about 2 to 3 times higher than that calculated by the reference response spectrum analysis (RSA). This includes the stack and the stairwell that nevertheless remain linear elastic in the non-linear transient analysis. This results from a conservative representation of structural damping (Rayleigh's method with low levels, see Section 4.2), in addition to the conservative nature of the seismic signals compared with the target spectrum.

Analysis of differentials displacement perpendicular to the expansion joints between structures shows that collisions may occur around the stack, the SE stairwell and the hot cell block.

4.3.2 – Overall loads

The paleo-earthquake generates the highest load, which occurs along the X-axis, while the highest loads along the Y and Z axis are generated by the safe shutdown earthquake. The masonry stiffness and strength assumption (minimum or maximum) had very little impact on the load level.

The maximum overall seismic load in the foundation slab represents 21% of the weight along the X-axis, 22% along the Y-axis, and 22% along the Z-axis. At level 0.00 m, this load represents 19% along the X-axis, 16% along the Y-axis and 22% along the Z-axis.

The seismic loads obtained by non-linear transient analysis for the X-axis exceed those calculated by modal spectrum analysis (between 13 and 28% depending on the case). This is surprising because it is generally understood that a non-linear transient analysis results in lower loads owing to the reduced stiffness and energy dissipation. This is due to the conservative modelling of the damping already mentioned in Sections 4.2 and 4.3.1.

The two approaches produce comparable loads along the Y-axis in the foundation slab. On level 0.00 m, however, the non-linear transient analysis calculates loads reduced by a factor of 0.64 for a safe shutdown earthquake and 0.53 for a paleo-earthquake. We can therefore see a significant decrease in the load due to the occurrence of dissipation mechanisms, mainly the plastic deformation of columns on the ground level.

4.3.3 – Analysis of the building's structural sensitivity to second-order effects

The building's structural sensitivity to second-order effects was analysed according the Eurocode 8-1 method (see Section 4.4.2.2(2) of NF EN 1998-1).

The ground floor was shown to be the most sensitive level along the Y-axis, exhibiting an overall plastic mechanism. The building structure proved to be sensitive to second-order effects for which the consequences were assessed by means of a simplified pushover analysis. Second-order effects lead to an increase in displacements by about 10%. However, we can consider that such displacement is covered by the conservative nature of the transient analysis.

Second-order effects are insignificant along the X-axis (north-south).

4.3.4 – Structural strength check of the main frame

4.3.4.1 - Material deformation

The maximum deformation of materials remains compatible with the structural behaviour requirements for the components (stability and/or support). However, the analysis of displacements and rotations revealed very significant deformations in some beams of the gable row 22 and in the masonry ground beams of rows 8, 11 and 14 between G and L, which could challenge their local stability.

4.3.4.2 - Strength of coupling devices

We checked that the maximum differential displacement in the coupling devices remained below their deformation capacity that was determined on the basis of test data. We also checked that the maximum loads transferred by the coupling devices remained below their structural strength taking into account interactions between the different components of the load. The analysis showed that the structural strength of all the coupling devices was demonstrated, except for the truck access airlock where the capacity is exceeded.

4.3.4.3 - Shear strength

By optimising the reinforcements to resist shear in the columns in compliance with the tests performed on strengthened samples, practically all of the columns met the shear strength requirements. Only six columns exceeded their shear strength: three columns significantly exceeded it while the other three only slightly.

4.3.4.4 - Column rotation capacity

Eurocode 8-3 was used to assess the rotation capacity of the columns on the ground level that undergo global plastic deformation. This capacity was compared with the maximum rotation so as to determine a safety factor $\gamma = \theta um / \theta max$. Eurocode 8-3 recommends a safety factor of 1.5. The safety factors we reached range between 1.3 and 3.8, with a mean of 2.1. Only four column configurations (out of a total of 36) reached a safety factor under 1.5, with a minimum of 1.3.

There is therefore no risk of seeing the columns collapse on the ground level.

We also covered the case of column sections in the hall with the highest rotation levels, including embedment with the beams on the upper flat roof. The resulting safety factor was at least 3.4.

4.3.4.5 - Masonry damage

With the most penalising assumption, 58 of the 120 masonry panels failed, i.e. about half. With the most advantageous assumption, only 8 panels failed, i.e. about 7%.

The most sensitive masonry panels were those on the ground level along the east-west axis. They failed every time, regardless of the configuration. These panels are used to close off the front area of the building.

The least-sensitive masonry panels were those along the north and south façade of the hall (rows D and G) between level +7 m (lower flat roof) and +13 m (upper flat roof). They practically all remained in place every time, regardless of the configuration.

This behaviour of the masonry panels explains why the structure undergoes extensive deformation along the east-west axis for the entire ground level, but much less so above this level.

4.3.4.6 - Strength of cover-strips

The allowable stress limit in the cover-strips was set at 292 MPa after the tests, incorporating a safety factor γ_{M2} = 1.25. The stress levels of the metal plates were assessed in all the strengthened areas containing cover-strips. The limit of 292 MPa is satisfactory in most cases, except in a few cases concerning five columns and a beam-wall. These cover-strips therefore need to be strengthened.

It should also be mentioned that the tests revealed a risk of embrittlement in the butt-welds between the 8 mm and the 4 mm metal plates, which will also require strengthenings.

4.3.4.7 - Analysis of portal frame beam-to-column connections

Four portal frame column-to-beam connections were chosen to analyse their structural strength in detail using a 3D non-linear solid model. The choice of connections was determined by: 1) analysis of the non-linear transient calculation results, which allowed us to identify the connections supporting the highest loads, and 2) the representativeness of these intersections in terms of the formwork, concrete reinforcement, and PHME strengthening's works.

The finite-element model of each connection took into account the related column and beam sections over a length that is 1.5 times the height of the section in question. The concrete was modelled in terms of solid elements defined by a 3D non-linear behaviour law. The rebars were modelled by rods, while the metal plates were modelled by multi-layer shell elements. Each steel grade (E24, S355, HA 400 and HA 500) was assigned a specific elastic-plastic behaviour law. The mesh size was about 2 cm. The loads on the connections were defined on the basis of the structure’s overall non-linear transient analysis results. The computing moments with the highest loads were chosen after having analysed the stresses in the different components connected to the connection in question. The concomitant stresses were applied to each section.

The main conclusion drawn from these calculations is that no failure mode was observed in the connections. The connections are therefore strong enough to allow a plastic mechanism to develop in the beam and column sections to which they are connected. The connections demonstrate sufficient robustness and do not represent a weak point in the structure.

Stress and strain were seen to be concentrated in specific areas in the concrete with respect to the usual uniaxial stress limits, but this could be justified by the triaxial behaviour of confined concrete.

4.3.5 – Analysis of foundation stability

High local uplift and stress was observed under the footings of the main columns in the hall (rows D and G). These phenomena, however, are not likely to call into question the stability of the building foundations.

The slip stability of most of the foundation footings was checked, except for column G16 and for the walls in rows L, 16 and 19. The risk of slip is nonetheless limited by the backfill soil, which hinders the displacement of buried walls, and by the foundation slab that redistributes some of the stress.

The strength of the building foundations on the micro-piles (strengthening added during the seismic renovation) is also confirmed.

4.3.6 - Conclusion

The stability of the overall structure is confirmed by the analyses for both a safe shutdown earthquake and a paleo-earthquake, but significant damage will occur. The following main issues have been identified:

- The risk of collision between some structures perpendicular to the expansion joints: stack, south-east stairwell, hot cell block along the east-west axis.
- The shear strength of six columns impacting limited areas
- The risk of instability in the gable of row 22 and in the masonry panels of rows J-L/8, 11 and 14
- The coupling system in the truck access airlock that exceeds its structural strength
- Some cover-strips used to connect reinforcing metal plates
- The analysis highlighted the conservative nature of some assumptions: modelling of damping and the seismic signals.

The local analysis of the most sensitive column-to-beam connections using 3D solid finite-element modelling shows that the connections do not represent a risk of structural embrittlement.

To conclude, the behaviour of the building structure is compatible with the performance requirements (stability and/or support) of the individual components, except for some local defects that must be resolved either by adding reinforcement or by analysing their consequences.

5. Programme of structural strengthening's works defined post-analysis

The works described below have been defined to meet the performance requirements to resist a safe shutdown earthquake and a paleo-earthquake.

5.1 – Widening of construction joints

Analysis has revealed the need to widen certain construction joints around the hot cell blocks (level +4.32 m), the stack (levels +4.25 m and +6.69 m) and the south-west stairwell/ lift (levels +3.36 m and +6.69 m).

5.2 – Improving the shear strength of hall's columns

Analysis also revealed that the shear strength of columns G4, G6, G20 and D14/D14' required strengthenings. This involves consolidating the transverse frames by inserting threaded rods right through the columns (according to the size of the cross sections) in holes drilled between the existing frames and reinforcements (metal plates) that were installed during the PHME renovation work. The threaded rods will be anchored to plates and sealed in the centre of the columns by injecting resin.

The reinforcements will be installed down the length of each column in which insufficient structural strength was detected by calculation.

5.3 – Strengthening of the gable in row 22

The non-linear transient analyses show that the gable beams in row 22 undergo significant plastic rotation and displacement mid-span to an extent that their local stability is not guaranteed when faced with out-of-plane bending loads. The strengthenings planned to resolve this issue are described in appendix 3.

5.4 – Strengthening of beams in the workshop area

For the load-bearing beams between rows J and L in front of rows 8/8', 11 and 14/14' (known as the workshop area beams), the issue is identical to that of the gable in row 22: these beams undergo significant plastic rotation and displacement at mid-span to the extent that their local stability is not guaranteed for out-of-plane bending loads. These beams overhang and support masonry walls defining the different rooms between rows 8/8' and 14/14'.

These beams will be reinforced by installing vertical risers on their surface to restrict any displacement or deformation associated with these beams.

IPE 300 was chosen as the structural steel section for row 11.

For rows 8/8' and 14/14' in front of which the masonry walls are doubled, the support structures are composed on two sets of IPE 300 steel sections.

5.5 – Strengthening of the truck airlock coupling system

The strength analysis of the components forming the truck access airlock's coupling device (longitudinal and transversal) shows that its weaknesses lie in:

- Combination of normal loads and high shear
- Insufficient shear strength owing to the off-centring between the anchoring and the deflection axis of the force.

The strengthening planned to resolve this issue are described in appendix 3.

5.6 – Strengthening of the stack

The stack is 34.80 m high and its base is at -4.80 m with respect to the laboratory's ground level (±0.00m).

The stack is made entirely from reinforced concrete and has a square-tube cross section with external dimensions of 1.90 x 1.90 m and internal dimensions of 1.60 x 1.60 m, i.e. 15 cm thick.

The stack is based on a 4.60 x 4.60 x 0.60 m footing and is connected to the floor on level ±0.00m.

The overall stability of the stack and the strength of the foundation footing have been validated.

Concerning the stack's bending capacity, the overall analysis of its main sections and local sections around openings made it possible to validate its strength.

In terms of its shear strength:

- The strength of the stack section above level ±0.00 m has been validated
- The stack section in the basement (-4.80 m > ±0.00 m) shows insufficient strength and therefore needs to be strengthened.

The concrete walls on the north and south sides of the stack need to made thicker by 50 cm, between the foundation footing and the underside of the floor on level ±0.00 m.

The additional thicknesses will be reinforced both vertically and horizontally, and then secured to:

- The existing stack's footing by embedding the vertical reinforcement bars comprising the reinforcement of the concrete thicknesses
- The existing stack's walls and floor beams on level ±0.00 m by embedding anchors.

6. Conclusion

The example given above shows how non-linear analysis can be used to represent the changes in both local and overall stiffness levels depending on the loading level. This type of analysis also indicates the related redistribution of loads, the energy dissipation mechanisms coming into play in the structure, and the effects of these phenomena on both the building's overall and local seismic responses. The interpretation of this analysis allowed us to define a suitable strengthening's programme for the building. More over this strengthening's programme is optimized compared to that which would have been defined on the basis of more conventional seismic assessments.

References

1) Guide ASN 2/01- Prise en compte du risque sismique à la conception des ouvrages de génie civil d'installations nucléaires de base à l'exception des stockages à long terme des déchets radioactifs
2) DTU P 18-702 - Règles BAEL 91 révisées 99 – Règles techniques de conception et de calcul des ouvrages et constructions en béton armé suivant la méthode des états limites
3) Eurocode 2 Design of concrete structures Part 1-1: General rules and rules for buildings
4) Eurocode 8: Design of structures for earthquake resistance Part 3: Assessment and retrofitting of buildings

Appendix 1 - Description of PHME strengthening's works

Eliminating the risk of interactions inside the building:

To avoid any contact between the hot cell blocks and the hall, the expansion joints on levels ±0.00 m and +4.32 m were widened to absorb the differential displacement calculated during the PHME studies.

The three main blocks of the building were also coupled (see Appendix 2) perpendicular to the expansion joints (20 mm wide) located along rows 8/8' and 14/14'.

Longitudinal coupling devices were installed at different levels (see below) to prevent displacement along the east-west axis:

- Beams of the lower (+6.69m) and upper (+13.85 m) flat roofs in rows D and G
- Beams supporting the travelling crane (+10.00m) in rows D and G
- Longitudinal beams at level with the lower flat roof (+6.69 m) in rows A, B, J and L.

Transversal coupling devices were installed at different levels (see below) to prevent displacement along the north-south axis:

- Slabs of the upper flat roof (+13.85 m)
- Slabs of the lower flat roof (+6.69 m)
- Floor slab on level ±0.00 m between rows A and D along the double rows (8/8' and 14 /14')

The underside of the roof of the truck access airlock was also coupled with row 22 (end of block 3), both transversally and longitudinally.

Eliminating loads and masses:

To reduce the horizontal loads:

- The backfill soil along the wall of row A has been removed down the length of the building to eliminate the horizontal pressure of the soil on the walls and portal frames
- The sloping concrete fill on the upper and lower flat roofs have been removed, therefore reducing the mass of the leaktight system to 30 kg/m² and the inertial forces under seismic conditions.

Eliminating rigid points:

The rigid points of the building's structure were eliminated as follows:

- The stairwell/lift have been disconnected from the structure on the technical levels and the flat roofs
- The stack has been disconnected from the rest of the structure from level ±0.00 m
- The non-reinforced concrete wall of row T has been disconnected from the rest of the building structure
- The masonry panels of the gables for rows 4 and 22, and the masonry panels in the rear area (between rows G and W) have been disconnected from the building's main frame.

Force restraint:

The beams of the floor on ±0.00m perpendicular to the small technical gallery (between rows G and J) have been extended on the south side using ground beams anchored by micro-piles in the rocky bund walls: the loads generated by a north-south earthquake are therefore transferred to level ±0.00 m on the row G side.

Increased structural strength:

Local reinforcements were installed to improve the strength and ductility of the components comprising the building's overall structural strength.

These reinforcements – mainly located on the columns and beams of the hall's portal frames (volume located between rows 4, 22, D and G) – have been designed to provide sufficient strength to resist a PHME without significantly increasing the initial structural stiffness.

The following principles were implemented:

- Reinforcement of the main column parts: 4 mm metal plates attached to the concrete with bolts to provide light support
- Reinforcement of beam-to-column connections at +13.00 m and longitudinal coupling devices: reinforced concrete stiffeners.

These reinforcements concern:

- Transversal portal frames of the gables for rows 4 and 22
- Transversal portal frames located on both sides to the expansion joints in rows 8/8' and 14/14'
- Several beam-to-column connections on level +13.00 m
- A few main transversal portal frames in specific locations
- A few columns in annexe areas.

Reinforcements were also implemented under the hall's slab on level ±0.00 m in the front area of hot cells 11 and 12 designed to receive heavy loads.

Strengthening and bonding after identifying the location of rebars in the concrete (red lines)

Bolting (embedding) and welding

Appendix 2

Description of the coupling devices used for the PHME strengthening's works

Longitudinal coupling devices:

Five types of longitudinal coupling devices were used:

- Type 1: two metal plates going through the expansion joint and attached to the ends of longitudinal beams on either side of the expansion joint. The metal plates are attached to the concrete by through-bolts or normal bolts.

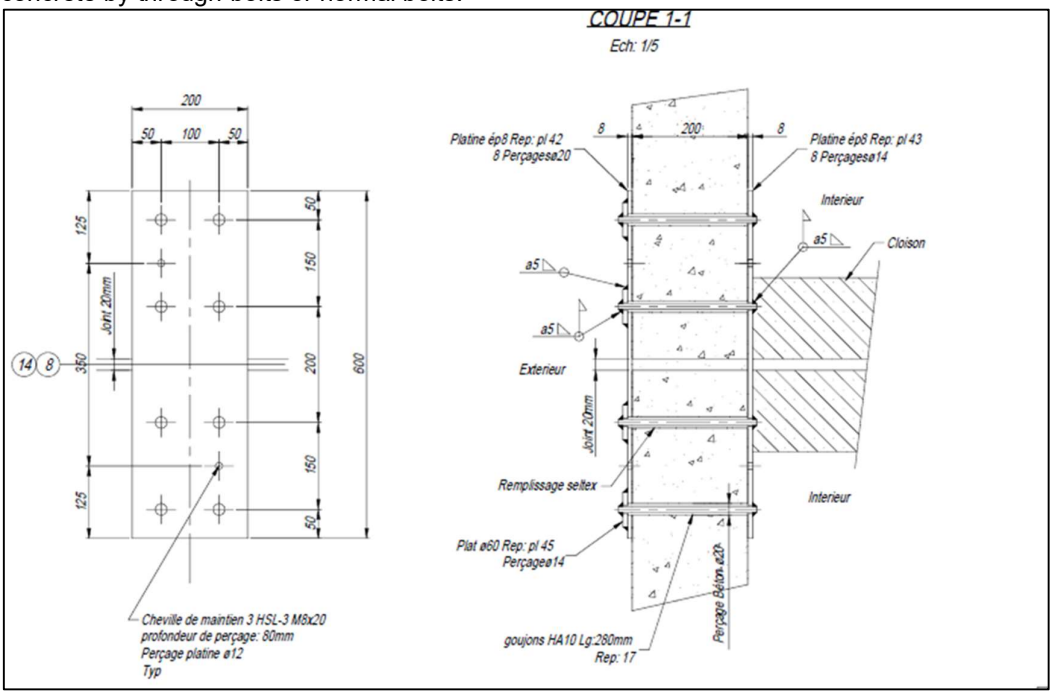

Example of a type-1 longitudinal coupling device

- Type 2: two indented steel reinforcement bars going through the expansion joint and the beams perpendicular to the longitudinal beams to be coupled. They are welded to two pairs of metal plates attached to the ends of the longitudinal beams by bolts.

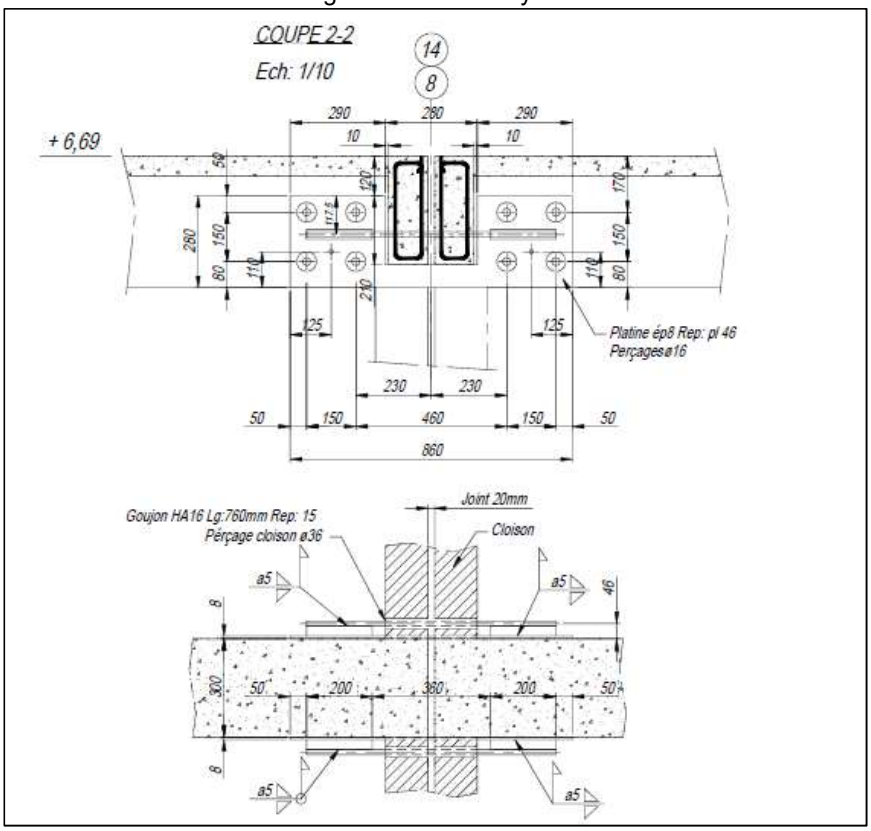

Example of a type-2 longitudinal coupling device

- Type 3: metal plate going through the construction joint and attached to the concrete by pins

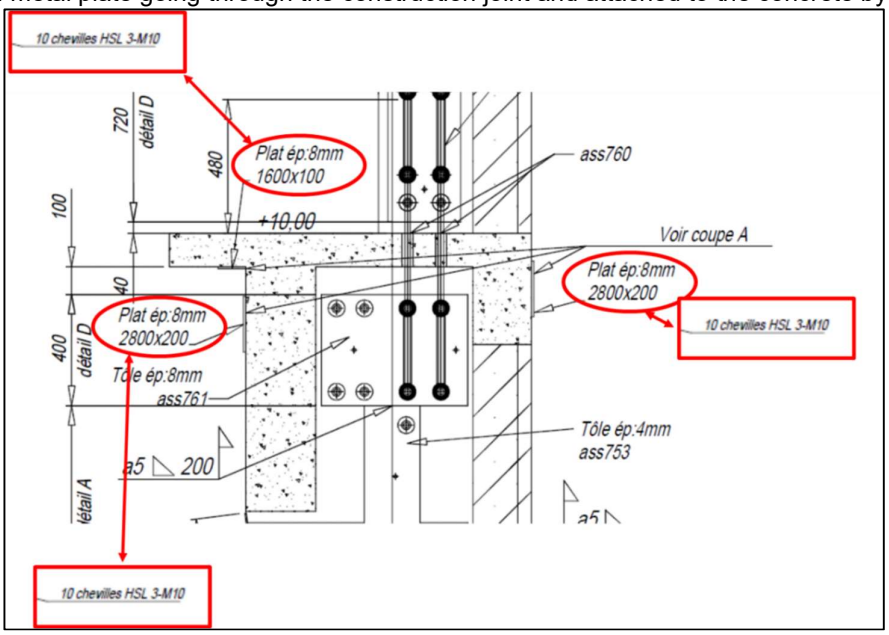

Example of a type-3 longitudinal coupling device

- Type 4: four deformed rods going through the expansion joint and welded to two metal plates attached to the concrete on the underside of the compression slab of the travelling crane girder. These metal plates are attached to the concrete with bolts.

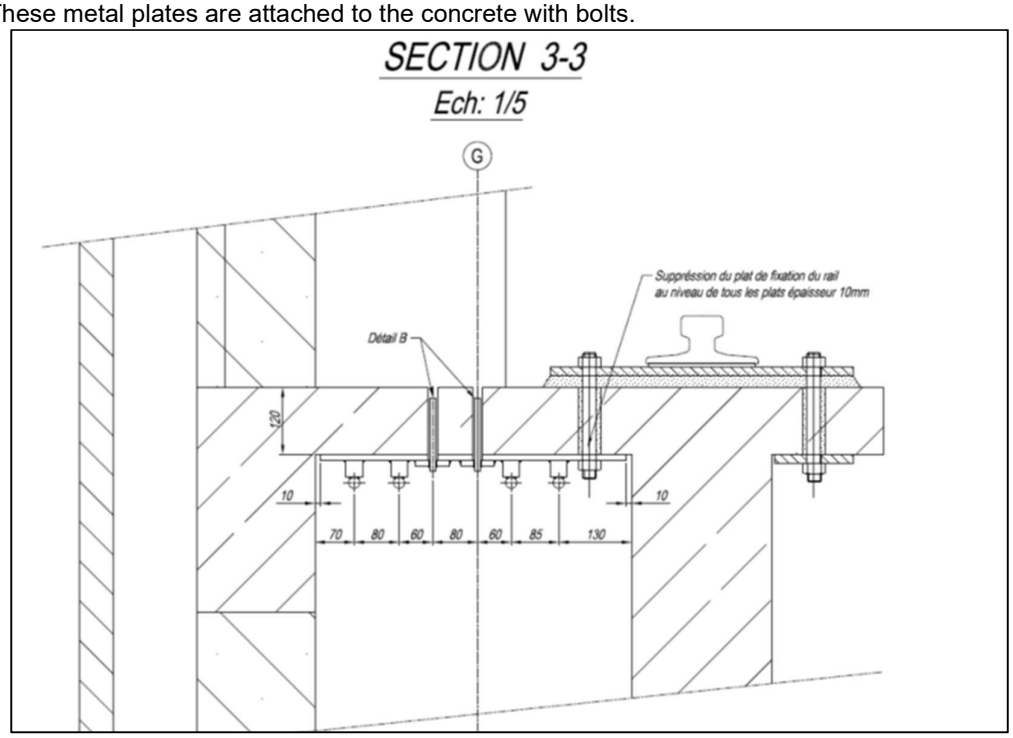

Example of a type-4 longitudinal coupling device

- Type 5: reinforced coupling device connected to the ends of reinforced concrete eave struts to be coupled

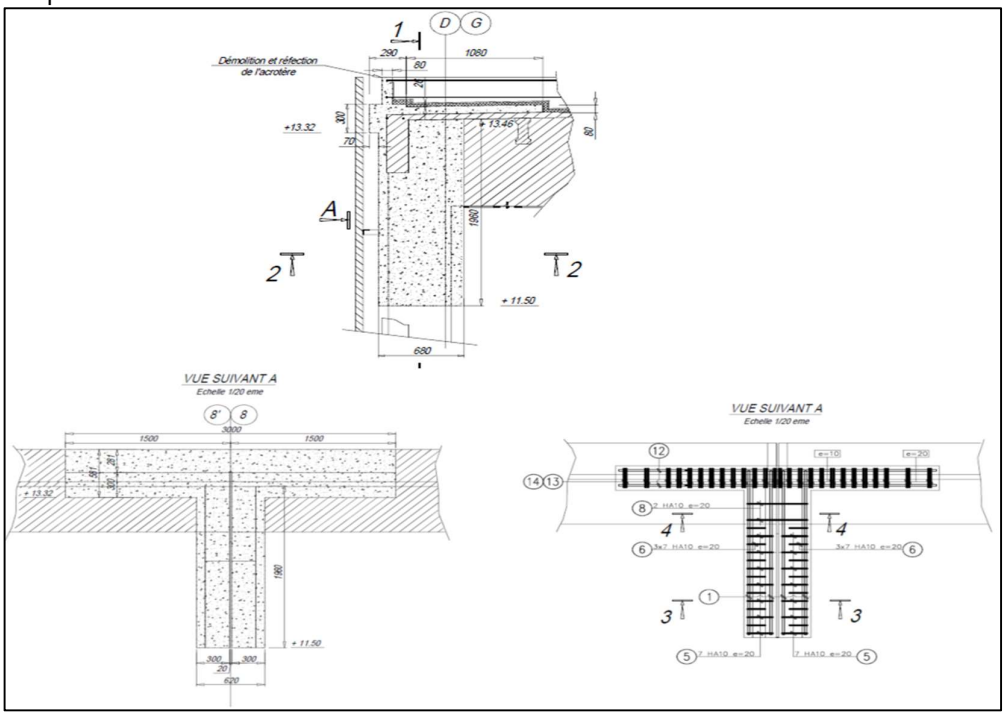

Example of a type-5 longitudinal coupling device

Transversal coupling devices:

The transversal coupling devices are composed of a series of twin plates 1.2 m long (length parallel to the joint) positioned on either side of the expansion joint between the blocks to be coupled. These plates are 290 mm wide (width parallel to the joint) and are attached to the concrete by through-bolts every 400 mm parallel to the joint. Metal plates with a width of 200 mm (width parallel to the joint) and a length of 600 mm (length perpendicular to the joint) are centred between these bolts. They are welded to one of the two plates of a block to be coupled and slide between pairs of stops (200 mm x 30 mm) welded to the other plate.

All these metal components are 8 mm thick.

This system operates much like two combs in staggered positions that prevent any north-south displacement.

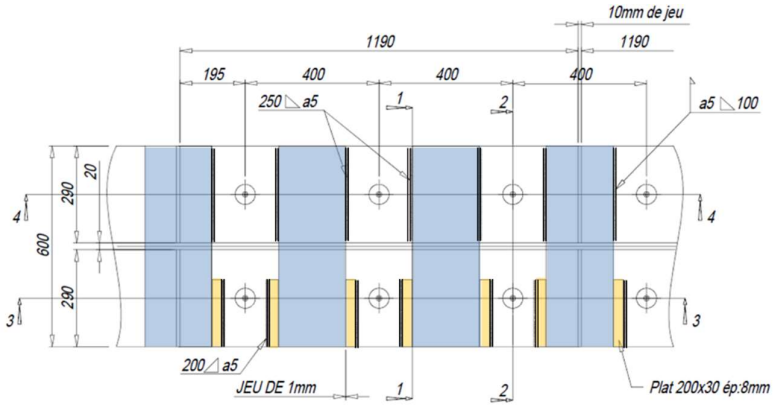

Plan view of a transversal coupling device

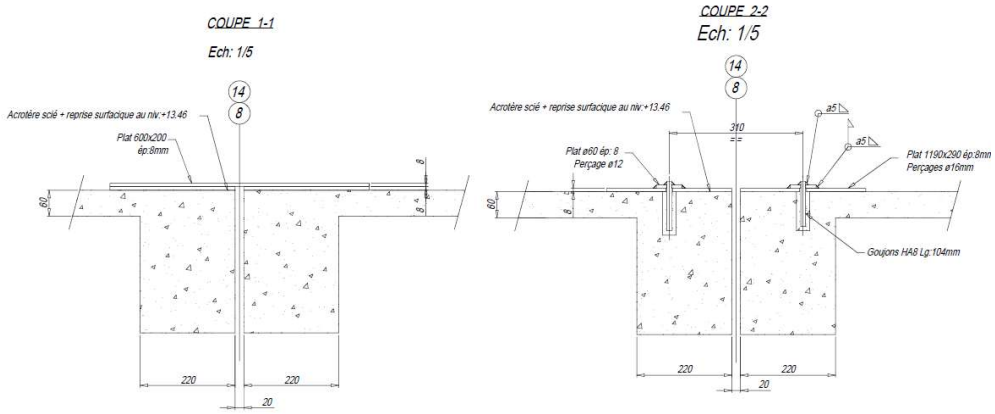

Cross-sections 1-1 and 2-2 of a transversal coupling device

Transversal and longitudinal coupling device for the truck airlock:

The longitudinal and transversal coupling of the truck airlock comprises two rows of metal sections (6 UAP) installed symmetrically on either side of the construction joint. The ends of the opposing metal sections are bolted together using a metal plate.

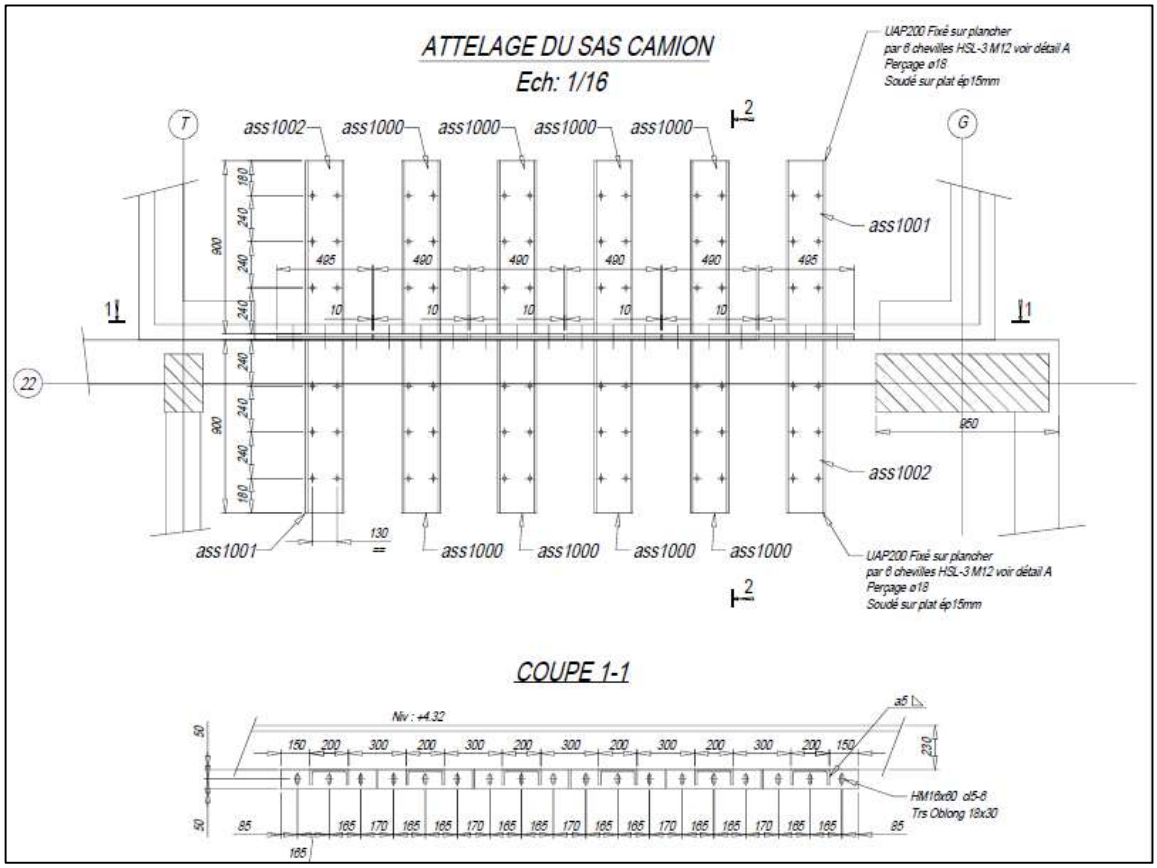
ATTELAGE DU SAS CAMION
Ech: 1/16
UAP200 Fixé sur plancher
par 6 chevilles HSL-3 M12 voir détail A
Perçage ø18
Soudé sur plat ép15mm
T
G
22
ass1002
ass1000
ass1001
ass1000
ass1000
ass1000
ass1000
ass1001
ass1002
ass1000
ass1000
ass1000
ass1000
UAP200 Fixé sur plancher
par 6 chevilles HSL-3 M12 voir détail A
Perçage ø18
Soudé sur plat ép15mm
COUPE 1-1
Niv : +4.32
HM16x80 cl5-6
Trs Oblong 18x30

Position of coupling devices

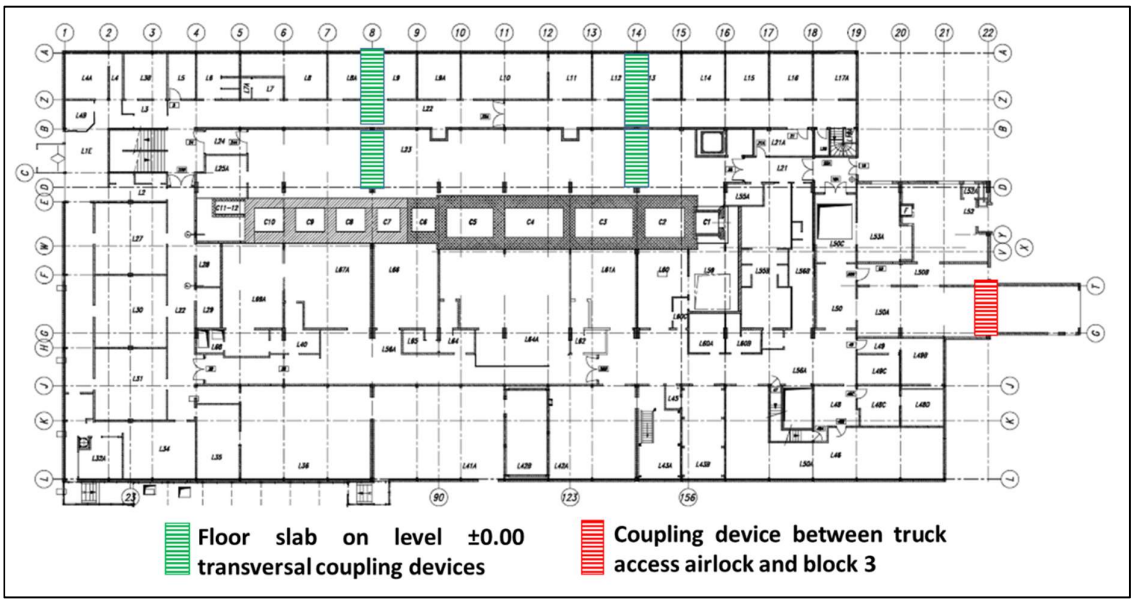

Layout of coupling devices on the ground level and in the truck access airlock

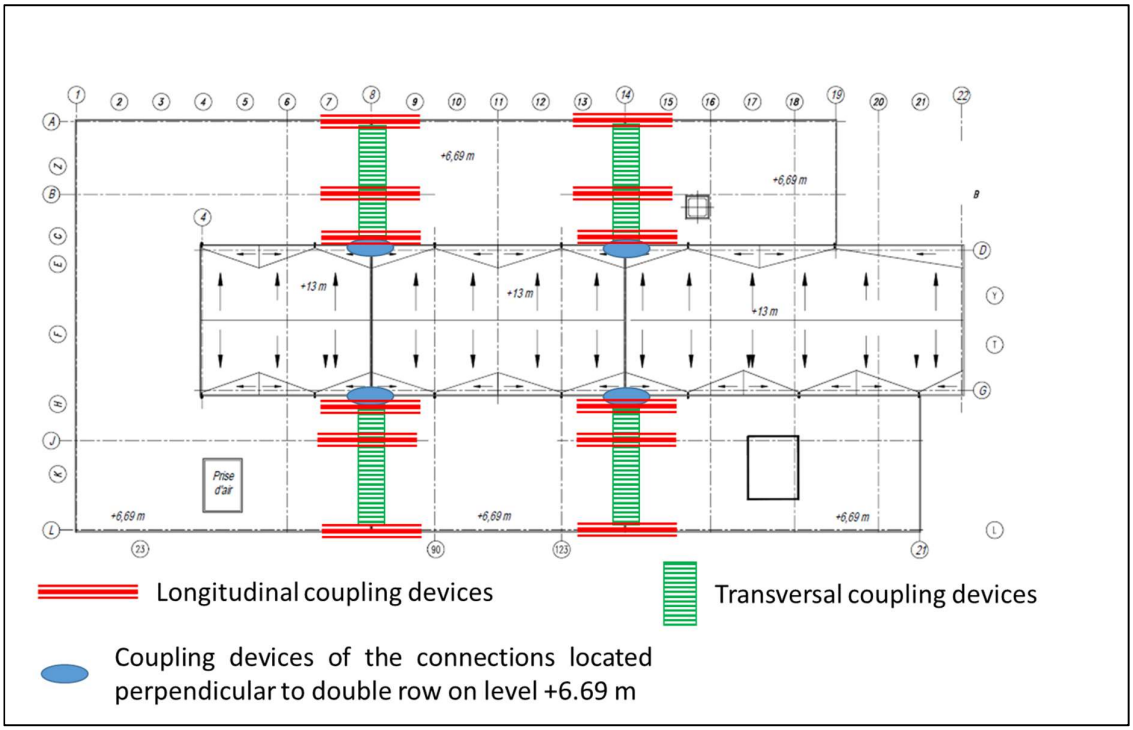

Layout of coupling devices on the lower flat roof level (+6.69 m)

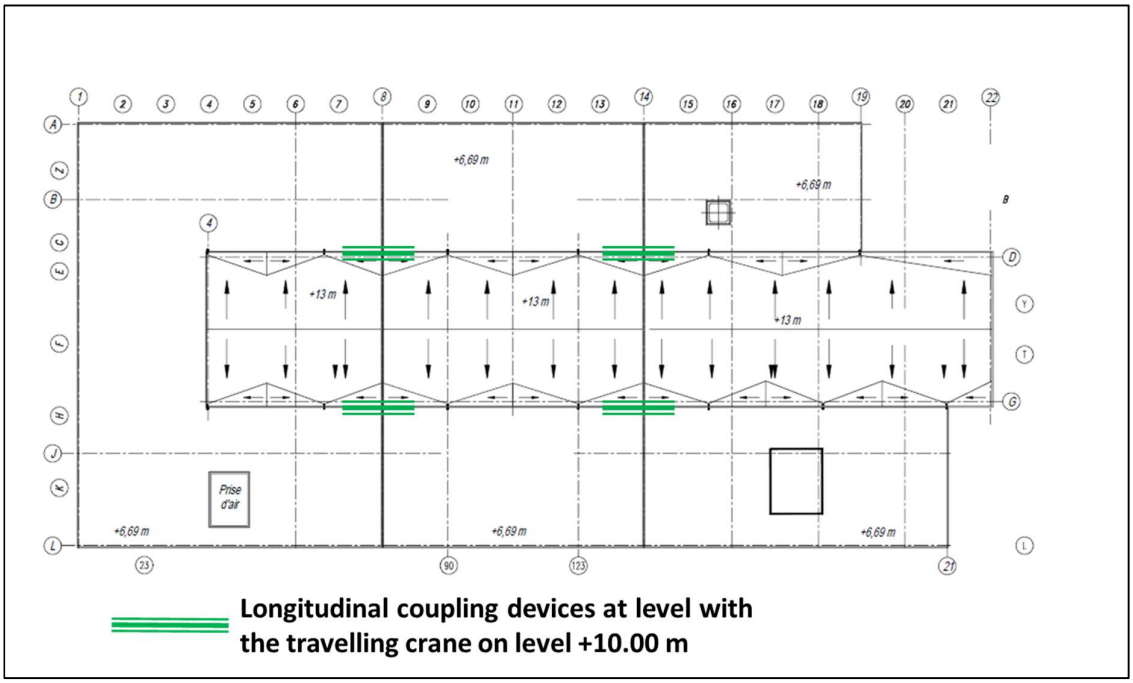

Layout of coupling devices on the travelling crane level (+10.00 m)

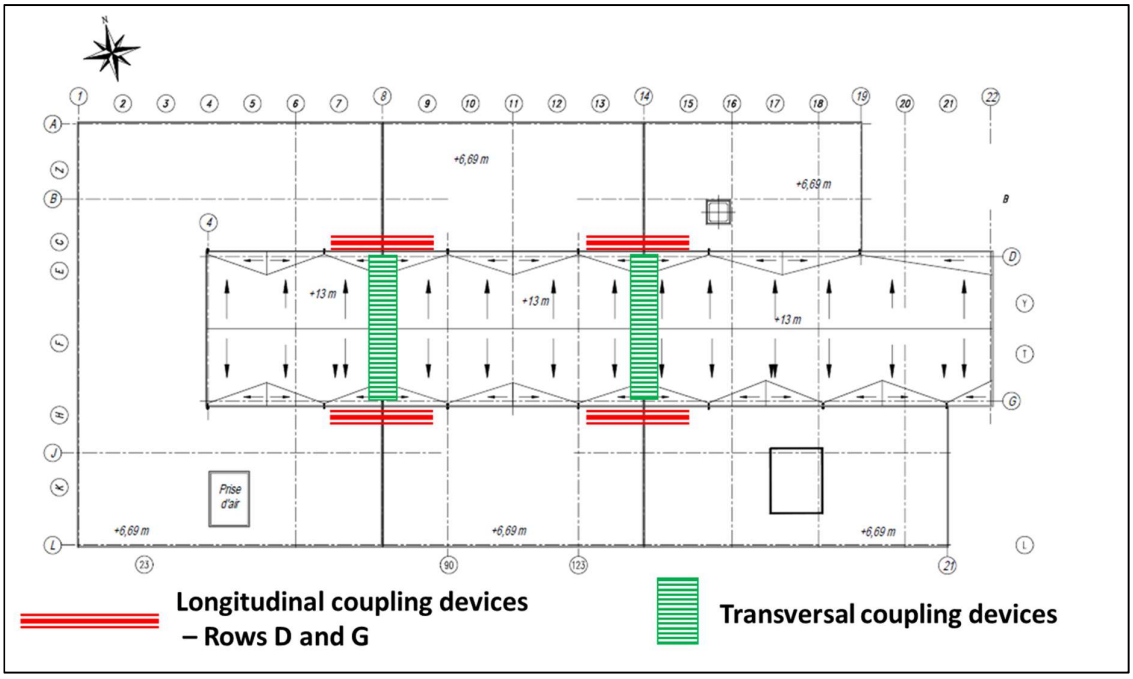

Layout of coupling devices on the upper flat roof level (+13.85 m)

Appendix 3

Strengthening's programme to meet safe shutdown earthquake & paleo-earthquake design requirements

Strengthening of the coupling device for the truck access airlock:

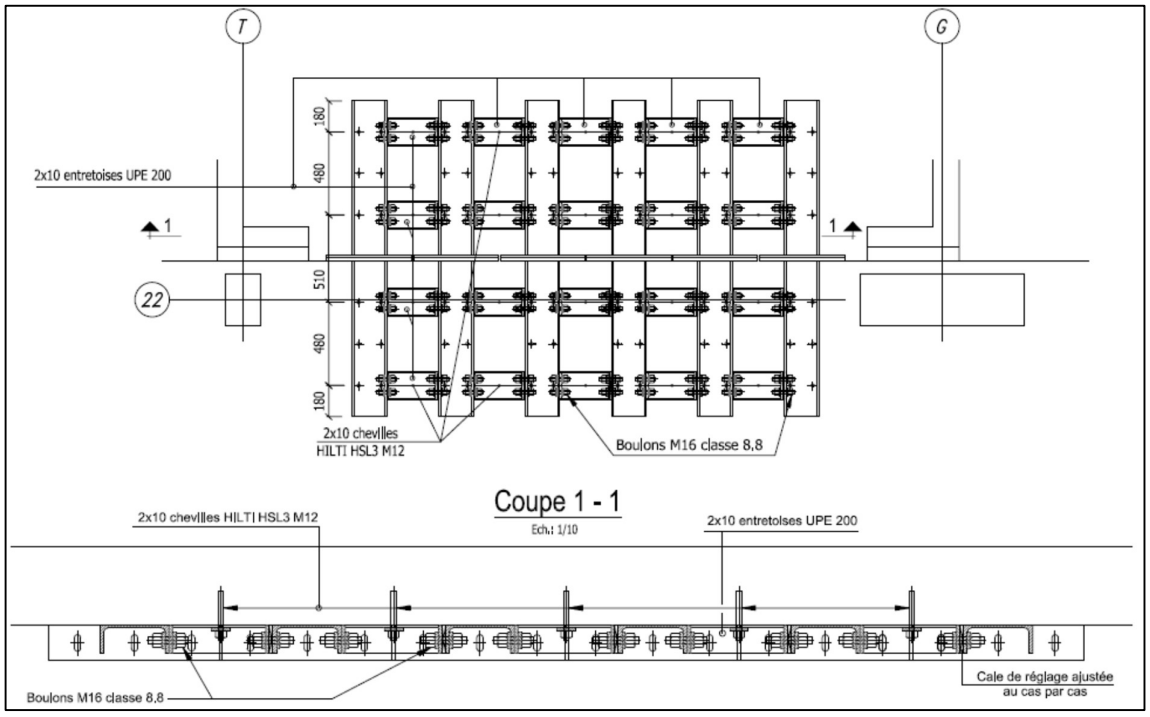

The solution chosen for the truck airlock coupling device involves linking the connection parts to impose monolithic behaviour for all of the sets of pins. Each UAP 200 metal section is connected to the neighbouring metal section by two spacers composed of UPE 200 sections: the moment resulting from the off-centring of the sets of pins with respect to the deflection axis of the shear force is therefore balanced out by the six sets of pins. This makes it possible to significantly increase the lever arm of force and reduce the loads in the pins. Each spacer is also pinned to the coupled reinforced concrete component.

Strengthening of the gable in row 22:

The reinforcement recommended for the beams in row 22 involves creating a metal frame applied to the external surface to stabilise these beams. This metal frame comprises a HEB 500 beam positioned horizontally on level +10.00 m. The HEB 500 beam is anchored to row 22 by two UPE 400 metal sections positioned horizontally and pinned to the side surfaces of the rolling beams in rows G and in row D. The ends of the HEB 500 beams are connected to the UPE 400 sections by threaded rods to form a hinge. Six vertical risers made from IPE 400 metal sections (simple support) are supported by the HEB 500 metal section. Each IPE 400 riser is also attached to the ground by a plate anchored to the concrete slab.

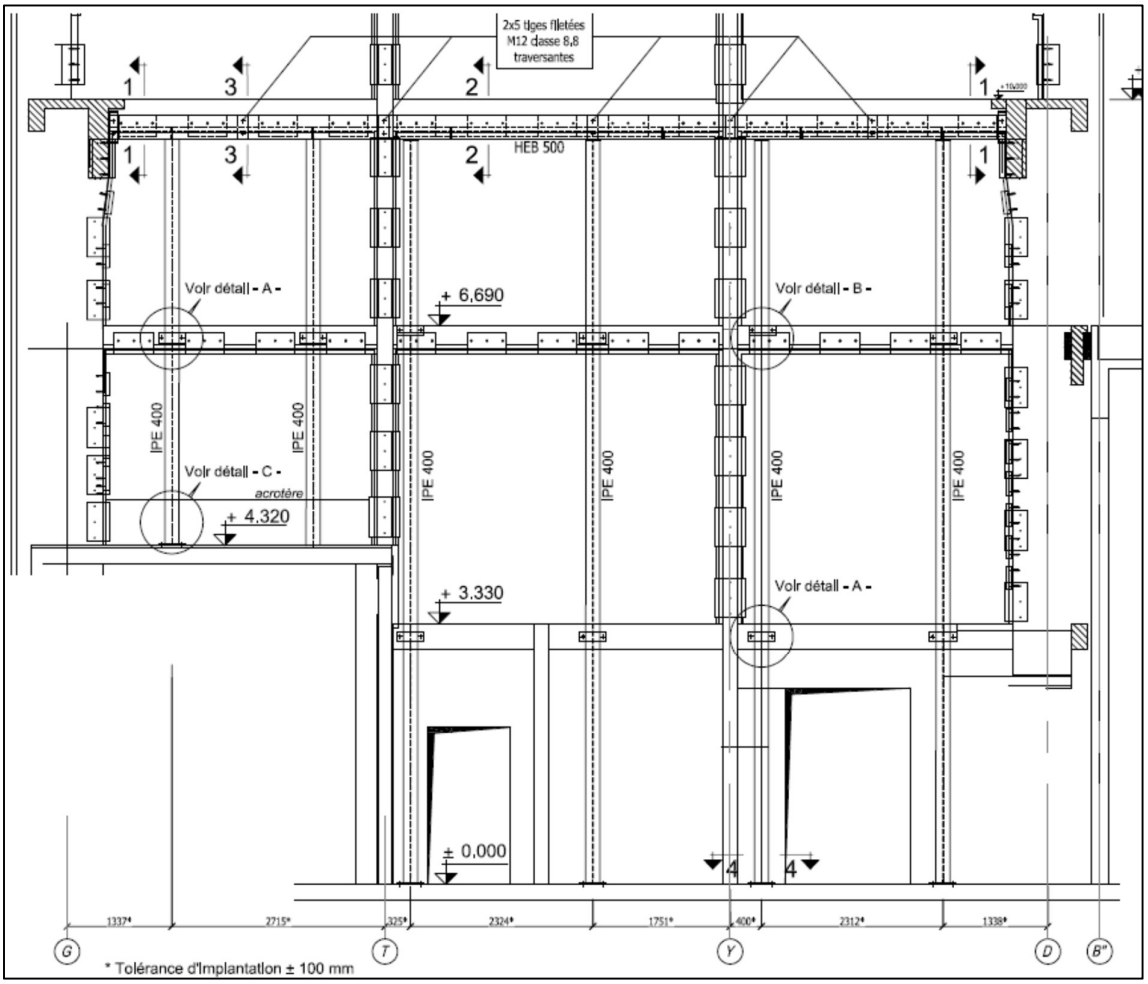

Strengthening of the gable in row 22